Quality Assurance and Safety of Crops & Foods, 2022; 14(2): 119–130

Ultrasound-assisted enzymatic extraction of soluble dietary fiber from fresh corn bract and its physio-chemical and structural properties

Ningning Geng[1,3], Jiangfeng Song[1,2,3*], Shuwei Luo[2], Ying Li[1], Gang Wu[4], Chunquan Liu[1], Caie Wu[2]

[1]Institute of Agro-Product Processing, Jiangsu Academy of Agricultural Sciences, Nanjing, China; [2]College of Light Industry and Food Engineering, Nanjing Forestry University, Nanjing, China; [3]School of Food and Biological Engineering, Jiangsu University, Zhenjiang, China; [4]Jiangsu Jia'an Food Co., Ltd., Nantong, China

***Corresponding Author:** Jiangfeng Song, Institute of Agro-Product Processing, Jiangsu Academy of Agricultural Sciences, Nanjing 210014, China. Email: songjiangfeng102@163.com

Received: 30 March 2022; Accepted: 19 April 2022; Published: 11 May 2022

OPEN ACCESS

RESEARCH ARTICLE

Abstract

The soluble dietary fiber from fresh corn bract (FCB-SDF) was extracted by ultrasonic-assisted cellulase method. The process parameters of FCB-SDF were optimized by Box–Behnken design (BBD), and the physio-chemical properties and structure of FCB-SDF obtained were investigated. The results showed that the optimal extraction conditions for FCB-SDF were enzyme concentration 1.58%, ultrasonic power 300 W, and extraction time 90 min. Under the above conditions, the FCB-SDF yield reached 21.21%. Compared with ultrasonic treatment group (U-SDF) and enzymatic treatment group (E-SDF), ultrasound-assisted enzymatic treatment group (UE-SDF) had higher WHC and OHC, but lower WSC. Its particle size was smaller, and a more microscopic pore structure was formed. UE-SDF had a low molecular weight of 204.41 KDa, and its monosaccharide composition had the highest arabinose content, followed by glucose. The SDFs obtained might be mainly composed of pectin and hemicellulose, E-SDF and UE-SDF contained more hemicellulose, and U-SDF contained more pectin.

Keywords: fresh corn bract; physio-chemical properties; soluble dietary fiber; structural characteristics; ultrasound-assisted enzymatic extraction

Introduction

Corn bracts are the outer bracts of the corn ears of the annual Gramineae Zea plant. They are not only the organs for photosynthesis and storage of photosynthetic products of corn plants but also provide high-quality living conditions for the growth of female ears (Mo, 2007). China is a large corn producing country globally. In 2019, China's corn output was as high as 260.77 million tons (Rui *et al*., 2021). The resources of corn bracts are abundant. According to statistics, about 600 kg of corn bracts can be harvested per hectare of corn (Xu *et al*., 2020). Several studies have found that corn bracts are rich in biologically active compounds including flavonoids, anthocyanins, polysaccharides, dietary fiber, as well as trace elements such as potassium, silicon, magnesium, and selenium. It has pharmacological effects on scavenging free radicals, regulating blood lipids, preventing atherosclerosis, lowering blood sugar, and inhibiting α-glycosidase (Gilbert and Liu, 2013; Masuoka *et al*., 2012). However, corn bracts are usually discarded, which cause serious waste of resources and environmental pollution (Luo *et al*., 2017). Overall, the utilization of corn bracts is still very low.

According to different dissolution characteristics, dietary fiber can be divided into soluble dietary fiber (SDF) and insoluble dietary fiber (IDF). It is suggested that SDF is the main contributor to the physiological functions of

dietary fiber. SDF has stronger physiological functions than IDF, such as the prevention and treatment effect on colon cancer, lowering blood cholesterol content, etc. (Jia *et al*., 2019; Madenci *et al*., 2018). Their uses are broader. Compared with IDF, SDF has greater solubility, viscosity, stronger water/oil holding capacity, and swelling capacity. SDF obtained from agricultural by-products is an excellent fat substitute. It can also increase the taste of various foods including dairy products, meatballs, and baked goods (Dong *et al*., 2020; Niu *et al*., 2020). Presently, the commonly used methods of extracting SDF mainly included chemical methods (acid-base treatment), and physical methods (extrusion, high-pressure homogenization, enzymatic hydrolysis, and fermentation). Among them, the enzymatic method has higher extraction rate and the reaction is gentler; in line with the theme of developing an environmentally friendly society, it has become a hot topic in the study of extracting SDF. Shi *et al*. (2007) used xylanase to hydrolyze corn seed coats pretreated by lipase, amylase, and protease to prepare water-soluble dietary fiber. The maximum yield of SDF was obtained by the optimal enzymatic extraction conditions and SDF mainly contained xylose, arabinose, galactose, and glucose. Mo (2007) prepared crude dietary fiber from corn bracts by enzymatic and chemical methods. In recent years, some auxiliary extraction methods have been gradually developed, including microwave, ultrasound, pressurization, and supercritical fluids (Gan *et al*., 2019). Among them, ultrasonic cell disruption technology could convert electrical energy into sound energy through a transducer, and this energy was changed by a liquid medium. The small bubbles were formed into dense small bubbles. These small bubbles burst rapidly to break the cells, increased the yield of soluble dietary cellulose, shortened the extraction time, and improved work efficiency (İşçimen and Hayta, 2018; Wu *et al*., 2020).

The current study therefore intended to optimize ultrasound-assisted enzymatic method to synergistically extract SDF from corn bracts. The effects of different extraction methods on the physicochemical properties, microstructure, and molecular composition of SDF in corn bracts were discussed, in order to provide data basis for the comprehensive utilization of fresh corn bracts resources.

Materials and Methods

Materials

Fresh corn bracts were obtained from Jiangsu Jia'an Food Co., Ltd (China). The samples were washed and drained, then were dried at 60°C until the moisture content was under 5%, crushed and passed through a 60-mesh sieve to obtain fresh corn bracts powder for use.

Dextran, mannose, arabinose, galactose, galacturonic acid, glucose, glucuronic acid, ribose, xylose, rhamnose, and fucose were purchased from Shanghai Yuanye Biotechnology Co., Ltd. 1-phenyl-3-methyl-5-pyrazolone (PMP) and cellulase (10,000 U/g, form *Trichoderma reesei*) were purchased from Shanghai Maclean Biochemical Technology Co., Ltd. Papain (≥2 million U/g, with casein as the substrate) was purchased from Shanghai Aladdin Biochemical Technology Co., Ltd. Trifluoroacetic acid, ethanol, acetone, hydrochloric acid, sodium hydroxide, and other reagents were all domestically manufactured and analytically pure.

Determination of the main chemical components in fresh corn bracts

The 105°C oven method was used to determine the moisture content of samples. The ash content in samples was determined by the combustion method. The Kjeldahl method was used to determine the protein content in samples with a conversion coefficient of 6.25. The Soxhlet extraction method was used to determine the fat content in samples. The enzyme gravimetric method was used to determine the dietary fiber content in samples.

Ultrasound-assisted cellulase extraction of FCB-SDF

An appropriate amount of fresh corn bract powder was weighed and mixed with distilled water according to a certain ratio of material to liquid ratio of 1: 20, and then 2% papain was added. After incubating for 60 min at 45°C, the enzyme was boiled and the precipitate was washed until the supernatant was colorless. The precipitate was dried and pulverized through a 40-mesh sieve.

Five grams of fresh corn bracts were dispersed in 0.02 mol/L phosphate buffer (pH 4.5), and an appropriate amount of cellulase was added. The liquid level in the flask was immersed below the water level in the ultrasonic instrument (KH-500DB Desktop CNC Ultrasonic Cleaner, Kunshan Hechuang Ultrasonic Instrument Co., Ltd. Jiangsu, China) for ultrasonic extraction, and the ultrasonic temperature was set to 50°C which was the optimum temperature for cellulase. After the extraction was completed, the precipitate was separated from the supernatant, and the supernatant was mixed with 95% ethanol in a mass ratio of 1:4. After alcohol precipitation at 25°C for 2 h, the precipitate was washed twice with 85% ethanol and acetone successively. The FCB-SDF obtained by the ultrasound-assisted enzymatic treatment group was named UE-SDF, the enzymatic treatment group was named E-SDF, and the ultrasonic treatment group was named UE-SDF.

The optimized experimental design of ultrasonic-assisted enzymatic extraction of FCB-SDF

Single-factor experiment

The amount of cellulase added (0.5, 1, 1.5, 2, and 2.5%), enzymolysis time (30, 60, 90, 120, and 150 min), ultrasonic power (200, 250, 300, 350, and 400 W), and the ratio of liquid to material (10: 1, 20: 1, 30: 1, 40: 1, and 50: 1 mL/g) were selected as the variables. The effects of cellulase addition, enzymolysis time, ultrasonic power, and liquid-to-material ratio on the yield of FCB-SDF were investigated.

Response surface optimization of ultrasonic-assisted cellulase extraction process for FCB-SDF

Based on the results of single-factor experiments, and according to Box–Benhnken's central combination experiment design principle, three factors that had a greater impact on the yield of FCB-SDF were selected: ultrasonic power, enzymolysis time, and the amount of cellulase added. FCB-SDF yield was taken as the response value. A BBD with 3 factors and 3 levels was performed. A confirmatory experiment was carried out based on the experimental results, and the yield of FCB-SDF was calculated. The design of factors and levels was shown in Table 1.

FCB-SDF physiochemical properties

Determination of water holding capacity, oil holding capacity, and water swelling capacity

Water holding capacity (WHC), oil holding capacity (OHC), and water swelling capacity (WSC) were determined according to our previous report by Geng *et al.* (2021).

Particle size distribution

The particle size distribution was determined by dynamic light scattering (Geng *et al.*, 2021). Dynamic light scattering measurement conditions: temperature was 23°C, laser wavelength was 633 nm, and scattering angle was 90°. The aqueous solution was used as the measurement medium, the viscosity was set to 0.933 cP, the refractive index was 1.333, the degree of the external fiber was 90°, and the measurement intensity was 300 kHz.

FCB-SDF microstructure

In order to evaluate the influence of different extraction methods on the microstructure of FCB-SDF, a scanning electron microscope analysis was carried out (Wu *et al.*, 2021b). The sample was placed on the double-sided tape on the sample stage, and after spraying gold, the image

Table 1. A Box–Behnken design scheme of ultrasonic-assisted enzymatic extraction of SDF from fresh corn bract.

Run	A: Ultrasonic power (W)	B: Enzyme concentration (%)	C: Extraction time (min)	The yield of FCB-SDF (%)	
				Actual value	Predicted value
1	0 (300 W)	0 (1.50%)	0 (90 min)	20.77 ± 0.13	20.84
2	−1 (250 W)	−1 (1.25%)	0	7.90 ± 0.21	7.82
3	0	0	0	20.60 ± 0.33	20.84
4	−1	0	−1 (80 min)	11.68 ± 0.18	11.84
5	1 (350 W)	0	−1	7.72 ± 0.16	7.76
6	0	0	0	20.96 ± 0.15	20.84
7	−1	0	1 (100 min)	10.23 ± 0.23	10.19
8	−1	1 (1.75%)	0	16.43 ± 0.25	16.38
9	1	1	0	12.77 ± 0.22	12.84
10	1	−1	0	9.87 ± 0.19	9.91
11	0	1	−1	11.83 ± 0.26	11.71
12	0	0	0	20.98 ± 0.14	20.84
13	1	0	1	12.98 ± 0.17	12.82
14	0	−1	1	7.56 ± 0.27	7.68
15	0	0	0	20.86 ± 0.11	20.84
16	0	−1	−1	6.68 ± 0.13	6.59
17	0	1	1	13.95 ± 0.27	14.04

was collected on the scanning electron microscope observation stage with an acceleration voltage of 10.0 kV, and the magnification was 1000 times.

Molecular weight distribution and monosaccharide composition of FCB-SDF

Using dextran as the standard, the molecular weight distribution of FCB-SDF was evaluated by gel exclusion chromatography (Chen *et al*., 2018). The sample was prepared into a 2 mg/mL solution, and then passed through a 0.45 μm microporous membrane to enter the HPLC instrument. The injection volume was 20 μL, the mobile phase was pH 6.7 phosphate buffers, the flow rate was 0.5 mL/min, the column temperature was set to 35°C, and the detector was a differential detector.

According to the method reported by Chen *et al*. (2018), the monosaccharide composition of SDF was determined. Hundred microliters of the hydrolyzed sample or monosaccharide standard was mixed with 100 μL of sodium hydroxide solution (0.6 M), and 100 μL of the mixed solution was added to the PMP-methanol solution (100 μL, 0.5 M), and mixed thoroughly with a vortex mixer. Then, the reaction was carried out at 70°C for 100 min. After the reaction solution was cooled to 25°C, 50 μL of hydrochloric acid solution (0.3 M) was added, and the mixture was rotary evaporated under reduced pressure at 50°C. It was then reconstituted with 1.0 mL of pure water, and the excess PMP in the solution was removed with chloroform. Finally, the samples were separated and peaks were quantified with HPLC instrument and Eclipse + C18 column (4.6 × 250 mm, 5 μm). The mobile phase was a mixture of phosphate buffered saline (PBS, 0.1 M, pH 6.7) and acetonitrile in a ratio of 83:17 (v/v). The injection volume was 20 μL, the flow rate was 1.0 mL/min, and the column temperature was 25°C.

Fourier transform infrared spectroscopy analysis of FCB-SDF

The wavelength was 400–4000 cm^{-1}, the number of scans was 32, and the resolution was 4 cm^{-1}. The air in the environment was used as a blank background for infrared measurement to determine the Fourier transform infrared spectrum (Wu *et al*., 2021a).

Statistical analysis

Each test was repeated thrice, and the results were expressed as mean ± standard deviation; SPSS 24 software and Design Expert 8.0.6 software were used to process the test data.

Results and Discussion

Chemical compositions of fresh corn bract

As shown in Supplementary Table 1, fresh corn bract dry powder mainly contained noncellulose carbohydrates (6.00% dm), protein (3.11% dm), moisture (3.65% dm), dietary fiber (85.21% dm), ash (1.55 % dm), and fat (0.47% dm). Its main ingredient was dietary fiber and the content was as high as 85.21%, which was significantly higher than the dietary fiber content in pear pomace (Yan *et al*., 2019) and rice bran (Azizah and Yu, 2000). It could be used as a good source of natural dietary fiber. The protein and a small amount of fat might interfere with the extraction of SDF. In this study, it was partially removed by enzymatic treatment.

The influence of enzyme concentration, liquid-to-material ratio, ultrasonic power, and extraction time on the yield of FCB-SDF

In Figure 1, as the cellulase concentration increased, the yield of FCB-SDF first increased and then decreased. When the cellulase concentration was 1.5%, the yield of FCB-SDF reached the maximum value of 18.39%. This was because when the enzyme dosage was lower, the contact between the enzyme and the substrate was insufficient. As the amount of cellulase increased, the contact area gradually increased, FCB-SDF was gradually extracted, and some IDF was cleavage into oligosaccharides and new chain ends, which increased the yield of FCB-SDF. When the enzyme concentration continued to increase, dietary fiber might be broken down into smaller monosaccharides and oligosaccharides (Chen *et al*., 2018), so that the yield of FCB-SDF was reduced.

It could be seen that as the liquid-to-material ratio increased, the yield of FCB-SDF increased first and then decreased. When the ratio of liquid to material was 30:1, the yield of FCB-SDF reached the maximum value of 15.40%. The reason might be that when the liquid-to-material ratio was relatively low, the concentration of the reaction system was high, the fluidity was poor, and the chance of contact between the substrate and the enzyme was reduced (Filgueiras *et al*., 2000). However, with the increase of the liquid-to-material ratio, the fluidity of the system increased, and the concentration difference between the enzyme in the solution and the boundary layer of fresh corn bracts increased, and the diffusion rate of FCB-SDF was faster. When the ratio of liquid to material was continuously increased, the probability of contact between the enzyme and the fresh corn bract powder decreased, and the yield of FCB-SDF decreased (Wu *et al*., 2020).

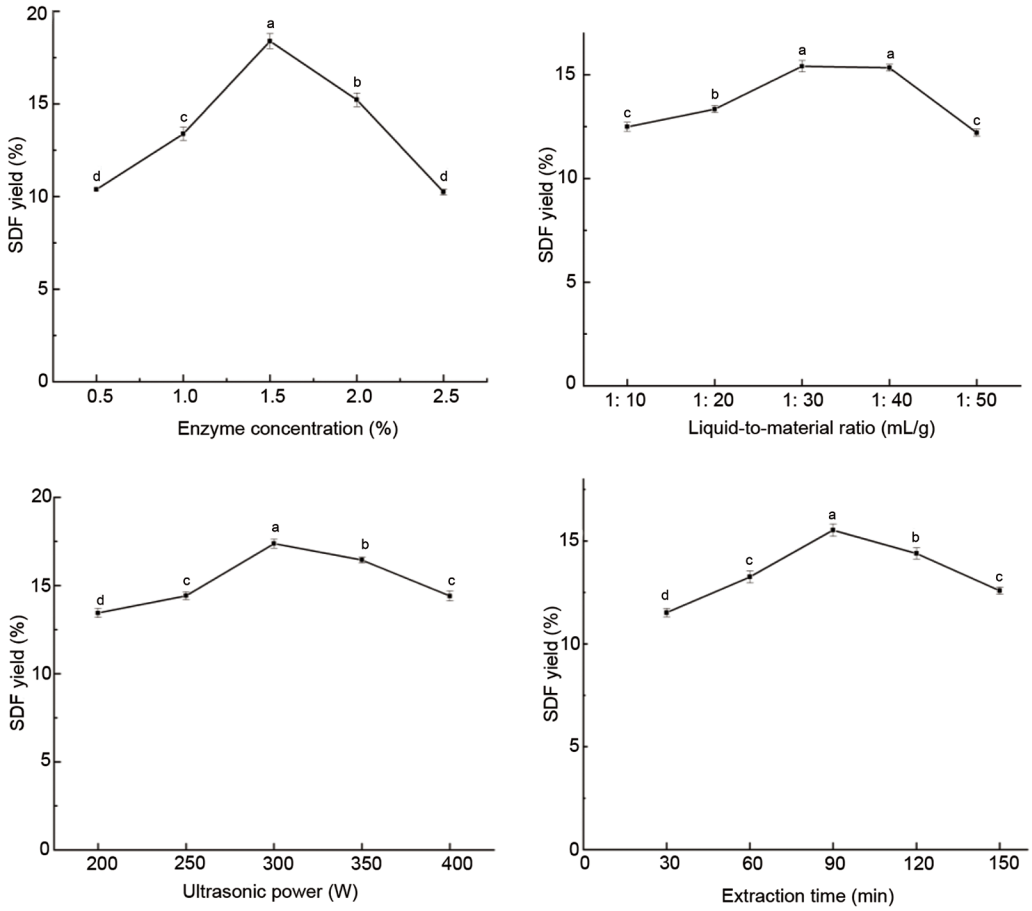

Figure 1. Effect of enzyme concentration, liquid-to-material ratio, ultrasonic power, and extraction time on the yield of FCB-SDF. Different letters under the same index indicate significant difference (P < 0.05).

As the ultrasonic power increased, the yield of FCB-SDF first increased and then decreased. When the ultrasonic power was 300 W, the yield of FCB-SDF reached the maximum value of 17.37%. The effect of ultrasound on the extraction process was mainly due to the vibration of the interface between the solvent and the solid substrate caused by ultrasound (Chen *et al*., 2012). For a given medium and fixed radiation area, the vibration was proportional to the ultrasonic power. The higher the ultrasonic power was, the stronger the vibration was, indicating that the increase in SDF extraction efficiency was caused by the increase in the number of cavitation bubbles and the increase in mass transfer rate. Therefore, an increase in power output would lead to an increase in extraction yield. On the other hand, under the action of ultrasound, the glycosidic bond between IDF in the dietary fiber might be broken, thereby converting IDF to SDF (Niu *et al*., 2020). When the ultrasonic power was greater than 300 W, it increased the number of cavitation bubbles in the solvent, which might reduce the efficiency of ultrasonic energy transmission to the medium. At the same time, high-intensity ultrasound caused FCB-SDF to crack and aggregate, which wouldill reduce the viscosity of the system resulting in a decrease in the extraction rate of FCB-SDF (Chen *et al*., 2012).

As the extraction time increased, the SDF yield first increased and then decreased. When the extraction time was 90 min, the yield of FCB-SDF reached the maximum. When the extraction time was longer than 90 min, the effect of cellulase and ultrasound caused SDF to decompose into small molecules, and the extraction yield decreased. These results can be explained as: on the one hand, ultrasound promoted mass transfer and made it easier for the solvent to come into contact with SDF. The cavitation effects such as the turbulence generated by the implosion of the cavitation bubble and the microjet generated by the cavitation on the product surface promoted the diffusion of SDF, which made the osmotic pressure inside and outside the cell different, so that the extraction of SDF quickly reached equilibrium. On the other hand, the prolongation of the ultrasonic time caused the expansion and collapse of the cavity near the cell wall and the turbulent vibration on the liquid–solid interface, leading to cell division and accelerating the release and diffusion of SDF from the cell wall into the water, thereby significantly increasing the extraction rate (Mehmet *et al*., 2020).

Response surface optimization of ultrasound-assisted enzymatic extraction of FCB-SDF

The FCB-SDF yield was the objective function to obtain the quadratic multiple regression equation: FCB-SDF yield (%) = $20.84 - 0.36 \times A + 2.87 \times B + 0.85 \times C - 1.41 \times A \times B + 1.68 \times A \times C + 0.31 \times B \times C - 4.22 \times A^2 - 4.87 \times B^2 - 5.96 \times C^2$.

Table 2 showed the analysis of variance of FCB-SDF extraction. It could be seen that the overall model F = 1659.17, P < 0.0001, the model was extremely significant, and the linear relationship between the dependent variable and the independent variable of the regression equation was obvious, indicating that this test method was reliable. The lack-of-fit item (F = 1.46, P = 0.35) was not significant, indicating the predicted value of the model could be in good agreement with the measured value. The adjustment coefficient $R^2_{Adj} = 0.9989$, indicating that 99.89% of the response value change could be explained by the model, and the correlation coefficient $R^2 = 0.9995$, indicating that the model fitted well with the experiment. Judging by the value of F, the influence of each factor on the yield of FCB-SDF was B = C > A, that was, enzyme concentration = extraction time > ultrasound power.

The Design Expert V8.0.6 software further analyzed the experimental data and calculated the fitted regression equation to predict the optimal process conditions for the ultrasonic-assisted enzymatic extraction of FCB-SDF. When the enzyme concentration was 1.575%, the ultrasonic power was 315 W, the time was 90.07 min, and the yield of SDF reached the highest with 21.32%. In order to check the accuracy, a verification experiment was carried out. The control enzyme concentration was 1.58%, the ultrasonic power was 300 W, and the time was 90 min. The SDF yield was 21.21 ± 0.11%, which was close to the predicted value, and the relative error was only 0.52%. It showed that the optimal process conditions obtained under this experimental model had high reliability. Moreover, the yield of SDF by ultrasonic-assisted enzymatic method was higher than that of ultrasonic method (15.25 ± 0.31%) and enzymatic method (14.00 ± 0.73%).

SDF physico-chemical properties

WHC, OHC, and WSC

The physico-chemical properties of SDF such as WHC, OHC, and WSC are important indicators to measure its physiological functions. The greater the WHC, OHC, and WSC was, the higher its physiological activity was (Jiang *et al.*, 2020). The WHC, OHC, and WSC of FCB-SDF samples obtained by different extraction methods were shown in Figure 2. The WHC (5.60 g/g) of UE-SDF was significantly higher than that of U-SDF (4.25 g/g) and E-SDF (3.78 g/g). The WHC of UE-SDF was higher than that of SDF in papaya peel (5.26 g/g) and orange peel (3.63 g/g). For OHC, UE-SDF (7.01 g/g) had the highest OHC compared to U-SDF (6.65 g/g) and E-SDF (6.28 g/g). Enzymatic hydrolytic modification cleaved the long chain and β-glycosidic bonds of SDF, thereby releasing hydroxyl groups that could be combined with water

Table 2. Variance analysis result of the regression equation for SDF extraction from fresh corn bract.

Source	Sum of squares	DF	Mean square	F value	P value	Significance
Model	454.01	9	50.45	1659.17	<0.0001	***
A-Ultrasonic power	1.05	1	1.05	34.48	0.0006	**
B-Enzyme concentration	65.97	1	65.97	2169.82	<0.0001	***
C-Extraction time	5.83	1	5.83	191.63	<0.0001	***
AB	7.93	1	7.93	260.70	<0.0001	***
AC	11.23	1	11.23	369.32	<0.0001	***
BC	0.39	1	0.39	12.66	0.0092	*
A^2	75.10	1	75.10	2470.15	<0.0001	***
B^2	99.91	1	99.91	3286.19	<0.0001	***
C^2	149.51	1	149.51	4917.55	<0.0001	***
Residual	0.21	7	0.03			
Lack of Fit	0.11	3	0.04	1.46	0.35	
Pure Error	0.10	4	0.03			
Cor Total	454.22	16				

Note: ***P < 0.0001, **P < 0.001, *P < 0.01.

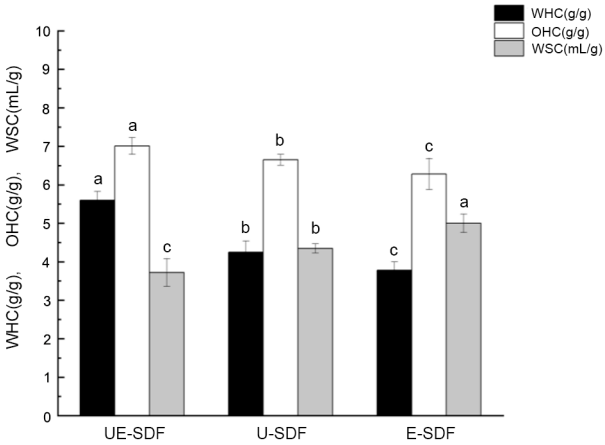

Figure 2. Effects of different extraction methods on WHC, OHC, and WSC of FCB-SDF.

(Liu *et al.*, 2020). The OHC of FCB-SDF samples were closely related to its hydrophobicity, surface properties, and total charge density. The high OHC of E-SDF might be because the enzymatic hydrolysis treatment increased the specific surface area of E-SDF to increase the contact area with oil. In addition, the exposure of more functional groups made it easier for oil and water to penetrate into DF molecules, which inevitably inhibited the loss of water and oil. The OHC of all FCB-SDF samples was higher than that of SDF in pear pomace (2.77g/g) and rice husk (1.85g/g). After enzymatic hydrolysis treatment and ultrasonic treatment, the change of the microstructure increased the surface area of the modified SDF, which in turn exposed more water binding sites, which was conducive for the absorption and penetration of water molecules. The improvement of UE-SDF's OHC could be attributed to the loosening of the structure and higher porosity after modification, which promoted its contact with oil. However, compared with UE-SDF (3.72 mL/g), E-SDF (5.00 mL/g) and U-SDF (4.35 mL/g) had significantly improved WSC. The WSC of E-SDF was similar to that of papaya peel SDF (4.05 mL/g) but lower than that of pear residue SDF (7.89 mL/g). IDF's WSC was affected by free hydroxyl groups and initial structural features (such as surface area, bulk, porosity, etc.).

Particle size analysis

The physicochemical and functional properties of fiber, such as water holding capacity, oil holding capacity, and the ability to transport and ferment in the colon, are closely related to its particle size (Huang *et al.*, 2021). As shown in Table 3, there were significant differences in the average particle size between UE-SDF, E-SDF, and U-SDF ($P < 0.05$). The effect of ultrasonic-assisted enzymatic treatment on the particle size reduction of SDF was more obvious than that of single enzymatic method or ultrasonic treatment. The polydispersity index of UE-SDF was smaller, which meant that the particle size was more concentrated. The cavitation effect of ultrasound could not only help extract dietary fiber but also destroyed the structure of SDF and reduced the size of dietary fiber. Both ultrasonic and enzymatic treatments reduced the particle size by destroying the structure of the original SDF. For enzymatic treatment, part of the structure was stretched after modification, and cellulase was more likely to come into contact with SDF, which might result in a smaller particle size of modified SDF. The particle size of E-SDF was larger than that of U-SDF, which might be due to the limited damage ability of single enzymatic treatment to fiber structure, while ultrasonic enzymatic co-processing usually produced SDF with relatively low molecular weight (Dong *et al.*, 2020).

Table 3. Molecular weight, particle size, and poly-dispersity index of FCB-SDF extracted by different methods.

Simple	Molecular weight (KDa)	Particle size (nm)	Polydispersity
UE-SDF	204.41 ± 10.07[b]	261.27 ± 3.80[b]	0.27 ± 0.01[b]
E-SDF	379.23 ± 9.99[a]	458.60 ± 8.23[a]	0.45 ± 0.03[a]
U-SDF	366.96 ± 11.45[a]	265.97 ± 2.85[b]	0.30 ± 0.04[b]

Note: Different letters in the same row indicate significant differences ($P < 0.05$).

Scanning electron microscope observation

The morphological characteristics of FCB-SDF samples were observed by SEM (Figure 3). The surface of E-SDF was relatively flat, with fewer cavities and larger particles. U-SDF had a relatively small particle size and honeycomb network structure. For UE-SDF, a cellular network structure with multiple folds and holes was observed. The three treatments resulted in extensive microscopic morphological differences. These changes indicated that the modification treatment had changed the structure of SDF and formed some valleys and cavities, which might lead to the exposure of more polar and nonpolar groups and the effective binding of cholesterol. The structure of UE-SDF became porous. It was possible that ultrasound-assisted enzyme treatment caused damage to the surface of the fiber matrix and exposure of the internal structure of the fiber, which easily formed a network with water and glucose molecules (Liu *et al.*, 2020; Zhang *et al.*, 2017). The change of the shape of SDF by ultrasonic-assisted enzymatic treatment was better than that of ultrasonic and enzymatic treatment, so that SDF could provide more space for storing water molecules by forming hydrogen bonds and dipoles (Liu *et al.*, 2020).

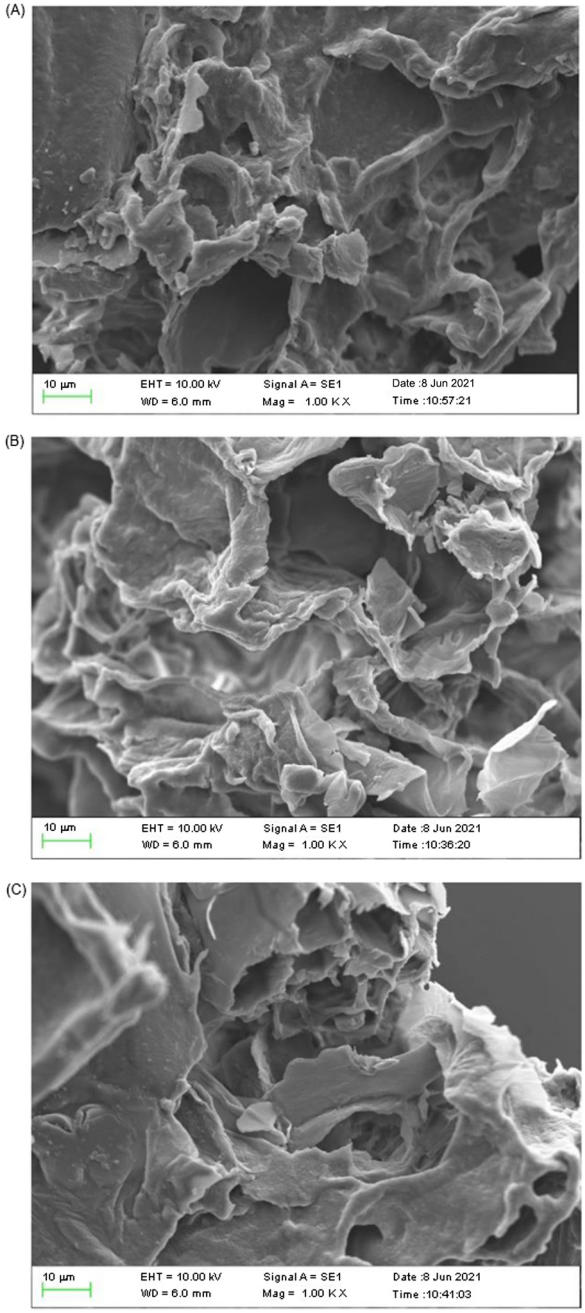

Figure 3. Effect of different extraction methods on the microstructure of FCB-SDF (× 1000 times). A: U –SDF; B: UE –SDF; C: E– SDF.

Molecular weight and monosaccharide composition

The molecular weights of SDFs prepared by different extraction methods had significant differences (Table 3). Compared with E-SDF (379.23 KDa) and U-SDF (366.96 KDa), UE-SDF had the smallest molecular weight (204.41 KDa). This might be due to the combined action of ultrasound and enzymes to break down the molecular chains of cellulose and hemicellulose, thereby reducing molecular polymerization (Dong *et al*., 2020). In addition, ultrasound destroyed the large molecular weights, resulting in the production of long-chain carbohydrates. Studies had shown that the molecular weight of SDF was closely related to its ability to bind cholesterol *in vitro*. Wolever *et al*. (2010) reported that compared with β-glucan with a higher molecular weight (about 500 KDa and 2 MDa), β-glucan with the lower relative molecular weight (about 200 KDa) had a stronger ability to lower blood cholesterol.

Table 4. Monosaccharide composition (mg/g) of FCB-SDF obtained by different extraction methods.

Simple (mg/g)	E-SDF	U-SDF	UE-SDF
Mannose	4.12 ± 0.12[b]	4.38 ± 0.22[a]	3.71 ± 0.21[c]
Ribose	5.46 ± 0.02[a]	4.75 ± 0.15[b]	4.62 ± 0.20[b]
Glucuronic acid	4.81 ± 0.10[b]	4.92 ± 0.01[b]	5.19 ± 0.99[a]
Galacturonic acid	36.49 ± 0.20[b]	37.73 ± 0.42[a]	37.35 ± 0.05[a]
Glucose	170.26 ± 0.90[a]	165.46 ± 1.91[b]	158.24 ± 0.19[c]
Galactose	55.29 ± 0.01[a]	48.73 ± 0.03[b]	44.71 ± 0.59[c]
Xylose	22.28 ± 0.02[b]	22.10 ± 0.01[b]	24.27 ± 1.7[a]
Arabinose	140.16 ± 0.20[b]	132.60 ± 0.20[c]	160.69 ± 0.02[a]
Fucose	10.56 ± 0.20[a]	8.09 ± 0.20[b]	10.61 ± 0.20[a]

Note: Different letters in the same row indicate significant differences ($P < 0.05$).

As shown in Supplementary Figure 1 and Table 4, the three SDFs were mainly composed of nine monosaccharides, including mannose, ribose, glucuronic acid, xylose, glucose, galacturonic acid, arabinose, galactose, and fucose. In enzyme treatment and ultrasonic treatment, the highest monosaccharide content was glucose, which reached 160.69 mg/g and 165.46 mg/g, followed by arabinose and galactose. Arabinose and galactose were the main components of pectin, which belonged to SDF. It might be that cellulase and ultrasound caused the glucose content of E-SDF and U-SDF to be more abundant than that of UE-SDF. The combination of ultrasonic treatment and cellulase hydrolysis resulted in the highest arabinose content in monosaccharides and the second reduction in glucose content. Ebringerova and Heinze (2000) found that the higher the arabinose content, the greater the solubility of the polymer.

Fourier transform infrared spectroscopy analysis

As seen in Figure 4, the absorption peak at 3287 cm^{-1} corresponded to the stretching of the hydrogen-oxygen bond (–OH), which was mainly derived from pectin (galacturonic acid) and hemicellulose (xylose, mannose,

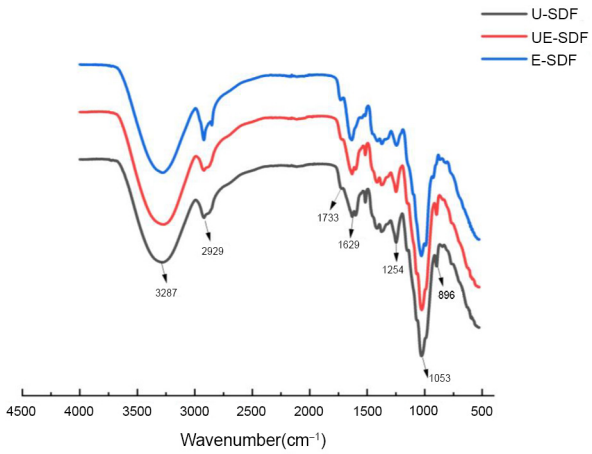

Figure 4. Effect of different extraction methods on the molecular structure of FCB-SDF.

galactose, and arabinose) (Wu *et al*., 2021; Zhang *et al*., 2017). Compared with E-SDF, the absorption peak intensities of the two SDFs were increased by ultrasonic treatment, which indicated that the two SDFs had more hydrogen bonds in the associated state (Li *et al*., 2019). The absorption band at 2929 cm^{-1} came from the vibration of the C-H bond (including C-H, $C-H_2$, and $C-H_3$), especially the stretching vibration of the methyl ester methyl group (CH_3), which was a typical structural absorption peak of polysaccharide compounds (Xu *et al*., 2015). The decrease or disappearance of the SDF peak intensity indicated that the extraction of SDF by enzymatic hydrolysis caused the partial degradation of methyl and methylene in the polysaccharide (Zhang *et al*., 2021). The main absorption at 1733 cm^{-1} corresponded to the stretching of the carbonyl group, indicating that more carbonyl groups and esters were formed in U-SDF. The absorption at 1629 cm^{-1} was due to the stretching of the carboxyl group, which was also a manifestation of the presence of crystal water in the sugar (Kan *et al*., 2021). The two peaks of carbonyl and carboxyl were the typical bonds for calculating the methoxy content of pectin, which indicated that U-SDF contained more pectin. The peak area was at 1200 cm^{-1} to 1420 cm^{-1}, reflecting the variable angle vibration of hydrocarbons (Xu *et al*., 2015). The absorption peak at 1254 cm^{-1} proved the presence of ester groups in pectin. Polysaccharides had typical absorption peaks in the range of 950 cm^{-1} to 1200 cm^{-1}, and the absorbance around 1053 cm^{-1} indicated the presence of a pyran ring structure in the molecule (Xu *et al*., 2015), namely, SDF was composed of pyranose monosaccharides. The absorption peak at 896 cm^{-1} was caused by D-glucopyranose (Mamun, 2005). Therefore, the three SDFs might be mainly composed of pectin and hemicellulose, E-SDF and UE-SDF might contain more hemicellulose, and U-SDF contained more pectin.

Conclusions

In this study, the SDF from fresh corn bract was extracted by ultrasonic-assisted cellulase method. The optimal extraction conditions for FCB-SDF were obtained through single factor test and BBD response surface experimental design method as follows: enzyme concentration 1.58%, ultrasonic power 300 W, and extraction time 90 min. Under the above conditions, the FCB-SDF yield was 21.21%, which was consistent with the experimental value. Compared with U-SDF and E-SDF, UE-SDF had higher WHC and OHC but lower WSC. Its particle size was smaller, and a more microscopic pore structure was formed. UE-SDF had a lower molecular weight of 204.41 KDa, and its monosaccharide composition had the highest arabinose content, followed by glucose. The SDFs obtained by the three extraction methods were mainly composed of pectin and hemicellulose, E-SDF and UE-SDF contained more hemicellulose, and U-SDF contained more pectin. The optimization of the ultrasonic and enzymatic extraction process of SDF from fresh corn bracts provided a good theoretical basis and data reference for the comprehensive utilization of waste corn bracts.

Acknowledgements

This work was supported by Primary Research & Development Plan of Jiangsu Province (Project number: BE2019324).

References

Azizah, A.H. and Yu, S.L., 2000. Functional properties of dietary fibre prepared from defatted rice bran. Food Chemistry 68: 15–19. https://doi.org/10.1016/s0308-8146(99)00145-4

Chen, G.J., Xie, M.H., Wan, P., Chen, D., Ye, H. and Chen, L.G., 2018. Digestion under saliva, simulated gastric and small intestinal conditions and fermentation in vitro by human intestinal microbiota of polysaccharides from Fuzhuan brick tea. Food Chemistry 244: 331–339. https://doi.org/10.1016/j.foodchem.2017.10.074

Chen, R.Z., Li, S.Z., Liu, C.M., Yang, S.M. and Li, X.L., 2012a. Ultrasound complex enzymes assisted extraction and biochemical activities of polysaccharides from Epimedium leaves. Process Biochemistry 47: 2040–2050. https://doi.org/10.1016/j.procbio.2012.07.022

Chen, X.J., Wu, X.F., Jiang, S.T. and Li, X.J., 2015. Applying response surface methodology to optimize extraction of soluble dietary fiber from pear residue using hemicellulose. Food Science 36: 18–23. https://doi.org/10.7506/spkx1002-6630-201506004

Dong, W.J., Wang, D.D., Hu, R.S., Long, Y.Z. and Lv, L.S., 2020. Chemical composition, structural and functional properties of soluble dietary fiber obtained from coffee peel using different extraction methods. Food Research International 136: 109497. https://doi.org/10.1016/j.foodres.2020.109497

Ebringerová, A. and Heinze, T., 2000. Xylan and xylan derivatives – biopolymers with valuable properties, 1. Naturally occurring xylans structures, isolation procedures and properties. Macromolecular Rapid Communications 21: 542–556. https://doi.org/10.1002/1521-3927(20000601)21:93.0.CO;2-7

Filgueiras, A.V., Capelo, J.L., Lavilla, I. and Bendicho, C., 2000. Comparison of ultrasound-assisted extraction and microwave-assisted digestion for determination of magnesium, manganese and zinc in plant samples by flame atomic absorption spectrometry. Talanta 53: 433–441. https://doi.org/10.1016/S0039-9140(00)00510-5

Gan, J.P., Huang, Z.Y., Yu, Q., Peng, G.Y., Chen, Y. and Xie, J.H., 2019. Microwave assisted extraction with three modifications on structural and functional properties of soluble dietary fibers from grapefruit peel. Food Hydrocolloids 101: 105549–105549. https://doi.org/10.1016/j.foodhyd.2019.105549

Geng, N.N., Song, J.F., Zhang, K.Y., Dai, Z.Q. and Li, D.J., 2021. Effect of dynamic high-pressure microfluidization on the physicochemical and structural properties of insoluble dietary fiber from fresh corn bract. Journal of Food Process and Preservation 45: 15710. https://doi.org/10.1111/jfpp.15710

Gilbert, E.R. and Liu, D., 2013. Anti-diabetic functions of soy isoflavone genistein: mechanisms underlying its effects on pancreatic β-cell function. Food and Function 4: 200–212. https://doi.org/10.1039/c2fo30199g

Huang, J.Y., Liao, J.S., Qi, J.S., Jiang, W.X. and Yang, X.Q., 2021. Structural and physicochemical properties of pectin-rich dietary fiber prepared from citrus peel. Food Hydrocolloids 110: 06140. https://doi.org/10.1016/j.foodhyd.2020.106140

İşçimen, E.M. and Hayta, M., 2018. Optimisation of ultrasound assisted extraction of rice bran proteins: effects on antioxidant and antiproliferative properties. Quality Assurance and Safety of Crops & Foods 10(2), 165–174. https://doi.org/10.3920/QAS2017.1186

Jia, M.G., Chen, J.J., Liu, X.Z., Xie, M.Y., Nie, S.Q., Chen, Y., Xie, J.H. and Yu, Q., 2019. Structural characteristics and functional properties of soluble dietary fiber from defatted rice bran obtained through Trichoderma viride fermentation. Food Hydrocolloids 94: 468–474. https://doi.org/10.1016/j.foodhyd.2019.03.047

Jiang, Y.L., Yin, H., Zheng, Y.R., Wang, D.F., Liu, Z.M., Deng, Y. and Zhao, Y.Y., 2020. Structure, physicochemical and bioactive properties of dietary fibers from akebia trifoliata (thunb.) koidz. seeds using ultrasonication/shear emulsifying/microwave-assisted enzymatic extraction. Food Research International 136: 109348. https://doi.org/109348,10.1016/j.foodres.2020.109348

Kan, J., Liu, J., Xu, F.F., Yun, D.W. and Yong, H.M., 2021. Development of pork and shrimp freshness monitoring labels based on starch/polyvinyl alcohol matrices and anthocyanins from 14 plants: a comparative study. Food Hydrocolloids 124: 107293. https://doi.org/10.1016/j.foodhyd.2021.107293

Li, L., Huang, L., Su, Y. and Fu, X.K., 2019. Structural characterization and functional properties of ultrafifine dietary fiber from phyllostachys praecox. Food Science 4: 74–81. https://doi.org/10.7506/spkx1002-6630-20180306-069

Liu, Y.L., Zhang, H.B., Yi, C.P., Quan, K. and Lin, B.P., 2020. Chemical composition, structure, physicochemical and functional properties of rice bran dietary fiber modified by cellulase treatment. Food Chemistry 342: 128352. https://doi.org/10.1016/j.foodchem.2020.128352

Luo, T.T., Tian, X.K., Yang, C., Luo, W.J., Nie, Y.L. and Wang, Y.X., 2017. Polyethylenimine – functionalized corn bract, an agricultural waste material, for efficient removal and recovery of Cr (VI) from aqueous solution. Journal of Agricultural and Food Chemistry 65: 7153–7158. https://doi.org/10.1021/acs.jafc.7b02699

Madenci, A.B., Bilgiçli N. and Türker, S., 2018. Effects of dietary fibre and antioxidant-rich ingredients on some quality characteristics of fresh and dry pasta. Quality Assurance and Safety of Crops & Foods 10(3): 315–324. https://doi.org/10.3920/QAS2018.1311

Mamun, A.M., 2005. Effect of drying methods on the functional properties of soy hull pectin. Carbohydrate Polymers 61: 362–367. https://doi.org/10.1016/j.carbpol.2005.06.009

Masuoka, N., Matsuda, M. and Kubo, I., 2012. Characterisation of the antioxidant activity of flavonoids. Food Chemistry 131: 541–545. https://doi.org/10.1016/j.foodchem.2011.09.020

Mehmet, Ü., Isil, I.G., Ersin, Ü., Mustafa, S.B., Kader, Ö.B., Aslı, S., Parvana, A., Namık, Ü., Osman, O., Hamdi, Ş. and Mahmut, K., 2020. Optimisation of biomass catalytic depolymerisation conditions by using response surface methodology. Waste Management and Research 38: 322–331. https://doi.org/10.1177/0734242X19890647

Mo, X., 2007. Study on the preparation of dietary fiber from corn bracts. Guangxi Journal of Light Industry (09): 24–25. https://doi.org/CNKI:SUN:GXQG.0.2007-09-011

Niu, X., Shi, Q.K., Zhao, C.B., Yin, H.H., Xu, X.Y. and Wu, Y.Z., 2020. Effects of ultrasonic modification on the physicochemical properties and structure of oat dietary fiber. Food Science 41: 1–7. Available at: http://kns.cnki.net/kcms/detail/11.2206.ts.20200302.1510.014.html

Rui, H.J., Liu, Y., Bai, Y., Yan, C.Y., Zhang, F. and Zhou, Y., 2021. Study on extraction and purification of flavonoids from corn – bract and its antioxidant activity. Farm Products Processing (03): 1–5. https://doi.org/10.16693/j.cnki.1671-9646(X).2021.02.001

Shi, C.B., Ma, Y.Q., Han, C.R., Sun, Z.Y., Li, X.M. and Cheng, L.M., 2007. Study on preparation of water – soluble dietary fiber of corn with Xylanase. Food Science (04): 123–127. https://doi.org/10.3321/j.issn:1002-6630.2007.04.025

Wolever, T., Tosh, S.M., Gibbs, A.L., Brand-Miller, J. and Wood, P.J., 2010. Physicochemical properties of oat β-glucan influence its ability to reduce serum LDL cholesterol in humans: a randomized clinical trial. American Journal of Clinical Nutrition 92: 723–732. https://doi.org/10.3945/ajcn.2010.29174

Wu, C.L., McClements, D.J., He, M.Y. and Li, Z., 2021a. Preparation and characterization of okara nanocellulose fabricated using sonication or high-pressure homogenization treatments, Carbohydrate Polymers 255: 117364. https://doi.org/10.1016/J.CARBPOL.2020.117364

Wu, F., Li, Z., Zhou, Q., Liu, C.H., Pan, M.Y. and Yu, D.Y., 2020. Study on ultrasonic-assisted aqueous enzymatic method extraction of rice germ oil and its component analysis. Food Science 41:233–241. Available at: https://kns.cnki.net/kcms/detail/11.2206.TS.20200831.1027.026.html

Wu, Y.J., Tang, P.Q., Quan, S.P., Zhang, H.Y., Wang, K. and Liu, J., 2021b. Preparation, characterization and application of smart packaging films based on locust bean gum/polyvinyl alcohol blend and betacyanins from cockscomb (Celosia cristata L.) flower. International Journal of Biological Macromolecules 191: 679–688. https://doi.org/10.1016/j.ijbiomac.2021.09.113

Xu, H.G., Jiao, Q., Yuan, F. and Gao, Y.X., 2015. In vitro binding capacities and physicochemical properties of soluble fiber prepared by microfluidization pretreatment and cellulase hydrolysis of peach pomace. LWT – Food Science and Technology 63: 677–684. https://doi.org/10.1016/j.lwt.2015.03.033

Xu, L., Zhao, J., Lu, B., Shi, Y. and Fan, Y., 2020. Current status and development trend of fresh corn seed industry in China. China Seed Industry 10: 14–18. https://doi.org/10.19462/j.cnki.1671-895x.2020.10.005

Yan, L., Li, T., Liu, C.H. and Zheng, L., 2019. Effects of high hydrostatic pressure and superfine grinding treatment on physicochemical/functional properties of pear pomace and chemical composition of its soluble dietary fibre. LWT – Food Science and Technology 107: 171–177. https://doi.org/10.1016/j.lwt.2019.03.019

Zhang, Q.Y., Zhang, S.K., Xi, L.Q., Du, H.Y. and Wu, P., 2021. Effects of different extraction methods on the structure, physicochemical and functional properties of water-soluble dietary fiber in cherry wine dregs. Food Science 42: 98–105. Available at: https://kns.cnki.net/kcms/detail/11.2206.TS.20200803.1442.064.html

Zhang, W.M., Zeng, G.L., Pan, Y.G., Chen, W.X., Huang, W.Y. and Chen, H.M., 2017. Properties of soluble dietary fiber-polysaccharide from papaya peel obtained through alkaline or ultrasound-assisted alkaline extraction. Carbohydrate Polymers 172: 102–112. https://doi.org/10.1016/j.carbpol.2017.05.030

Supplementary

Supplementary Table 1. The basic composition of fresh corn bract.

Composition	Water content	Ash content	Carbohydrate	Protein	Fat	Dietary fiber
Content (%, dry matter)	3.65 ± 0.32	1.55 ± 0.13	6.00 ± 0.21	3.11 ± 0.22	0.47 ± 0.15	85.21 ± 0.41

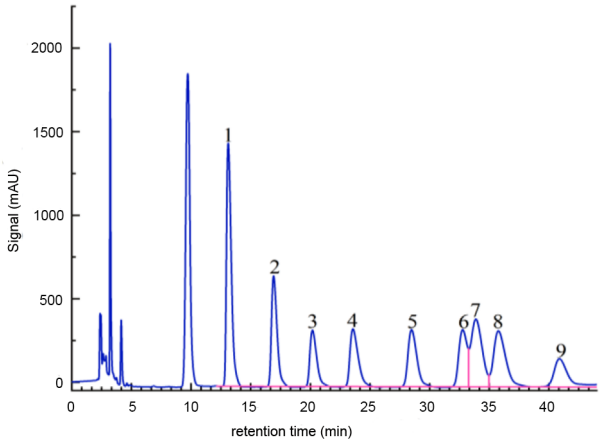

Supplementary Figure 1. Liquid chromatogram of monosaccharide standards. 1-Mannose, 2-Ribose, 3-Glucuronic acid, 4-Galacturonic acid, 5-Glucose 6-Galactose, 7-Xylose, 8-Arabinose, 9-Fucose.